Published in final edited form as:
Gastroenterology. 2009 September ; 137(3): 965–97610. doi:10.1053/j.gastro.2009.05.043.

Changes in mucosal homeostasis predispose NHE3 knockout mice to increased susceptibility to DSS-induced epithelial injury

Pawel R. Kiela[1,2,*], **Daniel Laubitz**[1,*], **Claire B. Larmonier**[1], **Monica T. Midura-Kiela**[1], **Maciej A. Lipko**[1], **Nona Janikashvili**[1], **Aiping Bai**[1], **Robert Thurston**[1], and **Fayez K. Ghishan**[1]

[1]Department of Pediatrics, Steele Children's Research Center, University of Arizona Health Sciences Center 1501 N. Campbell Ave, Tucson, AZ 85724

[2]Department of Immunobiology, University of Arizona Health Sciences Center, 1656 E. Mabel Street, Tucson, Arizona, 85724

Abstract

Background & Aims—NHE3 is a target of inhibition by proinflammatory cytokines and pathogenic bacteria, an event contributing to diarrhea in infectious and idiopathic colitis. In mice, NHE3 deficiency leads to mild diarrhea, increased intestinal expression of IFN-γ, and distal colitis, suggesting its role in epithelial barrier homeostasis.

Aim—To investigate the role of NHE3 in maintaining mucosal integrity.

Methods—Control or DSS-treated, 6–8 wk wild-type (WT) and NHE3$^{-/-}$ mice were used for the experiments. Small intestines were dissected for further analysis.

Results—NHE3$^{-/-}$ mice have elevated numbers of CD8α^{+} T and NK cells in the IEL and LPL compartments, representing the source of IFN-γ. NHE3$^{-/-}$ mice display alterations in epithelial gene and protein expression patterns which predispose them to a high susceptibility to DSS, with accelerated mortality resulting from intestinal bleeding, hypovolemic shock, and sepsis, even at a very low DSS concentration. Microarray analysis and intestinal hemorrhage indicate that NHE3 deficiency predisposes mice to DSS-induced small intestinal injury, a segment never reported as affected by DSS, and demonstrate major differences in the colonic response to DSS challenge in WT and NHE3$^{-/-}$ mice. In NHE3$^{-/-}$ mice, broad spectrum oral antibiotics or anti-asialo GM1 antibodies reduce the expression of IFN-γ and iNOS to basal levels and delay, but do not prevent, severe mortality in response to DSS treatment.

Conclusion—These results suggest that NHE3 participates in mucosal responses to epithelial damage acting as a modifier gene determining the extent of the gut inflammatory responses in the face of intestinal injury.

Introduction

Diarrhea is a common feature of inflammatory bowel diseases (IBD), occurring in approximately 50% of acute flare-ups of Crohn's disease (CD) and in virtually all patients with ulcerative colitis (UC)[1] and microscopic colitis[2]. The demonstrated severely diminished or reversed Na^{+} absorption in the colonic mucosa of CD and UC patients[3, 4] could be restored by steroid administration[5]. More recent studies determined that a

Correspondence: Fayez K. Ghishan, Department of Pediatrics, Steele Children's Research Center, University of Arizona Health Sciences Center; 1501 N. Campbell Ave., Tucson, AZ 85724. Phone: (520) 626-5170; Fax: (520) 626-4141; fghishan@peds.arizona.edu.

*Both authors equally contributed to this publication

Financial disclosures: All authors declare that there is no conflict of interest to disclose.

combination of epithelial barrier dysfunction and altered electrolyte movement account for the changes in net water flux during inflammation-associated diarrhea[6, 7]. Impaired expression and/or function of NHE3, the major mediator in the intestinal electroneutral Na^+/H^+ exchange, have been postulated to significantly contribute to chronic inflammation-associated and infectious diarrhea. Two key proinflammatory cytokines associated with intestinal inflammation, TNFα and IFN-γ[8, 9], have been demonstrated to inhibit NHE3 expression and/or activity, whereas anti-inflammatory agents as glucocorticoids[10, 11] or butyrate[12] significantly stimulate it. More recently, it was demonstrated that expression and activity of NHE3, as well as of the binding partners essential for its function are significantly diminished in IBD patients[13, 14]. Moreover, *Clostridium difficile* toxin B[15] as well as enteropathogenic *Escherichia coli* strains cause significantly depress NHE3 activity[16].

NHE3-deficient mice exhibit mild chronic diarrhea, distention and retention of alkaline fluid in all intestinal segments, mild metabolic acidosis and lower blood pressure[17]. Woo et al.[18] described a significant increase in expression of IFN-γ and IFN-γ-inducible genes, including iNOS, in the small intestinal mucosa of NHE3 knockout mice. Recently, we demonstrated that loss of NHE3 activity in $NHE3^{-/-}$ mice results in mild to moderate distal colitis with symptoms which could be alleviated by broad-spectrum oral antibiotics[19]. Microarray analysis correlated with these morphological findings and identified dysregulated genes not only consistent with altered nutrient transport, but also in response to an inflammatory insult and other key cellular processes[19]. This novel finding may be of great importance to the pathogenesis of IBD or infectious colits, where the degree of inhibition of NHE3 expression and/or activity, combined with genetic predisposition of the host, may influence the degree and extent of inflammation and/or mucosal restitution.

The aim of this study was to investigate the effect of NHE3 deficiency on mucosal homeostasis in a well defined model of DSS-induced mucosal injury. As we demonstrate in this report, NHE3-deficient mice display changes in the intraepithelial and lamina propria $CD8\alpha^+$ T and NK cell populations which represent the source of IFN-γ. $NHE3^{-/-}$ mice also display alterations in epithelial gene and protein expression patterns which predispose them to an extremely high susceptibility to DSS, with high and accelerated mortality, even at a very low DSS concentration, and rapid death resulting from a combination of intestinal bleeding, hypovolemic shock, and sepsis. Microarray analysis indicated that NHE3-deficiency predisposes mice to DSS-induced small intestinal injury, a segment never before reported as affected by DSS. These results strongly suggest that NHE3 participates in mucosal responses to epithelial damage and may act as a modifier gene determining the extent of the gut inflammatory responses in the face of intestinal injury.

Methods

Animals

Slc9a3 null knockout mice ($NHE3^{-/-}$) and their WT littermates ($NHE3^{+/+}$) were bred on the mixed genetic background (129/Black Swiss) whereas *Slc9a2* knockout mice ($NHE2^{-/-}$) as well as WT littermates ($NHE2^{+/+}$) were bred on the Non-Swiss Albino background. Detailed description is provided in the Supplementary Material. All animal protocols and procedures were approved by the University of Arizona Animal Care and Use Committee. Detailed description of tissue collection for analyses, including immunohistochemistry and in-situ hybridization is provided in the Supplement.

Isolation of intraepithelial and lamina propria lymphocytes, magnetic sorting and flow cytometry

IEL and LPL isolation, sorting and flow cytometric analyses are detailed in the Supplement.

Hematology

Hematology profile analyses with full differential were done by an experienced pathologist at the University Animal Care Pathology Services, the University of Arizona using the Hemavet 850 Mascot (Drew Scientific, Farmington, CT).

Real-time RT-PCR

Expression of selected genes was independently analyzed by real-time RT-PCR using TaqMan technology and commercially available primers as described in detail in the Supplement.

Western blot analysis

Expression of phospho-Stat1 (pY701), total Stat1, and Glyceraldehyde 3-phosphate dehydrogenase (GAPDH) was evaluated in the small intestinal epithelium as described in detail in the Supplement.

Immunohistochemistry and transmission electron microscopy (TEM)

Tissue preparation and detailed description of immunofluorescent staining is provided in the Supplement.

In-situ hybridization (ISH)

ISH was performed using Ultra-sensitive In situ Hybridization Detection Kit with specific biotinylated DNA probes (both from MBI) according to the manufacturer's protocol (see Supplementary Methods)

Histological evaluation

Sections of the proximal and/or distal colon and ileum were deparaffinized and rehydrated by use of standard procedures. For histological analysis, standard hematoxylin and eosin (H&E) staining was performed and digitally documented as described for ISH.

Intestinal permeability

Mucosal tracer flux was analyzed *in vivo* using two different markers: fluorescein isothiocyanate-labeled dextran (FITC-dextran; average M.W. 4,000) and FITC-labeled 5-(and-6)-sulfonic acid, trisodium salt (FITC-SA; M.W. 478.32) as described in the Supplementary Methods.

Nitric oxide determination

To determine the ileal NO content, we utilized the Nitric Oxide Quantitation Kit (Active Motif, Carlsbad, CA) based on nitrate and nitrite determination after enzymatic conversion, as described in the Supplementary Methods.

Microarray analysis of colonic gene expression

These studies were performed with Affymetrix GeneChip Mouse Genome 430 2.0 arrays (Affymetrix, Santa Clara, CA) and are described in detail in the Supplementary Methods.

Statistical analysis

Unpaired Student's t-test or ANOVA followed by post hoc Fisher's protected least significant difference (PLSD) test were used for all comparisons, with $P \leq 0.05$ considered significant. Data are expressed as means ± SD. Statistical analysis of microarray data was performed as described in the Supplementary Methods.

Results

Elevated expression IFN-γ and IFN-γ signaling is accompanied by an increased expression of iNOS, increased NO production, but by a paradoxical downregulation of endothelin-1 in NHE3$^{-/-}$ mice

IFN-γ and iNOS mRNA expression was significantly elevated in the small intestinal mucosa of NHE3$^{-/-}$ mice, with a concomitant increase in the ileal NO concentration (Suppl. Fig. 1). We investigated the phosphorylation status of Stat1 on tyrosine 701, an event critical for its homodimerization, nuclear translocation and activation of type II interferon-inducible genes. Western blotting indicated a significant activation of Stat1, and its elevated expression, confirming the positive autoregulatory loop of the Jak/Stat machinery described in other systems (Suppl. Fig. 2).

Contrary to the known stimulatory effects of cytokines and NO on the expression of endothelin-1 (ET-1), its expression was reduced by nearly 90%, and 35% in the small intestine and colon of the NHE3$^{-/-}$ mice, respectively (Suppl. Fig. 1). This finding suggests aberrant intestinal microcirculation in the absence of NHE3, and may partially explain intestinal hemorrhage in response to mucosal injury as described later in this report.

Localization of IFN-γ-expressing cells in the small intestinal mucosa of NHE3-deficient mice

Microarray analysis identified 1,688 probe sets representing 1,256 non-duplicated and well-annotated genes with expression altered ≥2-fold (t-test $p \leq 0.05$) in NHE3$^{-/-}$ mice compared to WT mice (Suppl. Fig 5A). In addition to a large number of genes from the transport GEO category (198 genes), we observed a remarkable induction of genes involved in antigen presentation, T cell activation, immune response, chemotaxis, response to wounding, leukocyte transendothelial migration, adhesion molecules, TLR-signaling, and apoptosis. (Suppl. Fig. 5 and Table 1). Both MHCI and MHCII pathways appeared to be induced, with their master regulators, NFYα and CIITA increased 2.6- and 2.2-fold, respectively. The small intestinal mucosal transcriptome of NHE3$^{-/-}$ mice was consistent with activation of CD8α$^+$ T or NK cells, both of which could serve as the primary sources of IFN-γ in NHE3$^{-/-}$ mice.

The yields of IEL and LPL from the same length segment were significantly greater in NHE3-deficent mice (Fig. 1A) and mononuclear cells of both fractions isolated from the NHE3$^{-/-}$ mice had significantly elevated expression of IFN-γ mRNA (Fig. 1A). Some of the early producers of IFN-γ, which could conform to our gene expression data, are NK cells and CD8α$^+$ T cells. Indeed, flow cytometry analysis of the intestinal LPL population demonstrated an increase in the contribution of CD8α$^+$ T cells in NHE3$^{-/-}$ mice (44.4% vs. 68.8%), which effectively translated into a dramatic increase in the absolute number of CD3ε$^+$/CD8α$^+$ cells (Fig. 1A). Among the magnetically sorted CD8α$^+$ T cells (98.5% pure), we also observed an increase in TCRαβ$^+$ natural memory T cells (46.1% vs. 82.2%; not shown). In both the unsorted LPL population, as well as in the magnetically sorted CD8α$^+$ T cells isolated from the small intestine of NHE3$^{-/-}$ mice, we identified a population of double positive CD8α$^+$ASGM1$^+$ cells consistent with the phenotype of the central memory T cells (T_{CM}) [20]. While the percentile contribution of CD8α$^+$/ASGM1$^+$

cells was not altered between genotypes, their absolute numbers also increased due to overall higher cell yield. We observed a two-fold increase in the intracellularly stained IFN-γ^+ cells among the magnetically sorted CD8α^+ lymphocytes (but not CD4$^+$; not shown) isolated from NHE3$^{-/-}$ mice and stimulated in vitro with PMA and ionomycin in the presence of brefeldin A (Fig. 1B). Within the magnetically sorted CD8α^- cells (Fig. 1A), as well as in the unsorted LPL cells (not shown), we also observed a significant increase in the number of ASGM1$^+$ NK cells

IFN-γ expression was not elevated in the Peyer's patches or mesenteric lymph nodes of NHE3$^{-/-}$ mice (not shown), and in situ hybridization for IFN-γ demonstrated a strong signal primarily localized to the lamina propria of the small intestinal mucosa (Fig. 2A). To test if the ASGM1$^+$ cells contribute to the production of IFN-γ and iNOS in the small intestinal mucosa of NHE3-deficient mice, WT and NHE3$^{-/-}$ mice were treated with immunodepleting anti-ASGM1 antibodies. As demonstrated in Fig. 2B, anti-ASGM1 antibodies completely eliminated the increase in IFN-γ and iNOS expression in NHE3 knockout mice, further suggesting that the primary source of IFN-γ in the small intestinal mucosa are ASGM1$^+$ cells.

Alterations in the apical junction complexes in the small intestinal epithelium of NHE3$^{-/-}$ mice

Despite no change in mRNA expression (not shown), occludin staining was diffuse and less punctuate and AJC-specific, while typical strong basolateral E-cadherin staining was significantly less evident and also more diffuse in the NHE3$^{-/-}$ mice (Fig. 3A). Microarray analysis demonstrated an ~2-fold reduction in β-actin mRNA (consistent with weaker staining for polymerized F-actin in NHE3$^{-/-}$ mice [Fig. 3A]), as well as a 2.76-fold increase in expression of claudin-2, verified by real-time RT-PCR (Fig. 3B). In the intestinal epithelium of NHE3-deficient mice, TEM indicated that significantly more AJC's were dilated (less tightly apposed) with higher frequency of AJC's with a loss of membrane kiss, as exemplified in Fig. 3C and summarized in Fig. 6A. These findings point to the role of NHE3 in the maintenance of epithelial integrity and cell-cell interactions. Consistently, when we isolated epithelial cells (IEC) from the same length segment of the small intestine, significantly greater (~6-fold) yield of IEC's was routinely obtained from NHE3$^{-/-}$ mice, as compared to WT animals (not shown). Morphometric analysis did not demonstrate significant differences in the villi length or crypt depth in WT and NHE3$^{-/-}$ mice (not shown). We have observed no significant increase in the epithelial cell apoptosis as evaluated by cleaved caspase-3 staining (Suppl. Fig. 3), or in situ oligo ligation (ISOL) assay (ApoptTag Assay, Millipore; [not shown]). Similarly, no significant changes were observed in the fraction of proliferating (Ki67$^+$) epithelial cells along the crypt-villus axis, with increased Ki67 staining in the infiltrating LPL cells (Suppl. Fig. 4).

High mortality of NHE3$^{-/-}$ mice in response to DSS

Kaplan-Meyer plot in Fig. 4A depicts the survival rate of NHE3$^{+/+}$ mice, NHE3$^{+/-}$, or NHE3$^{-/-}$ mice to increasing concentrations of DSS over seven days. Both 1% and 4% DSS treatment resulted in 100% mortality within five days. WT mice demonstrated 95% survival during 7 day DSS exposure. DSS concentration as small as 0.5%, normally ineffective in normal mice, also induced dramatic mortality in NHE3-deficient mice. All NHE3$^{-/-}$ mice rapidly developed wasting disease with accelerated body weight loss. Within two days of DSS treatment, vast majority of NHE3-deficient mice developed watery diarrhea with frank blood in their stools, and frequent rectal prolapse. None of the symptoms were observed in WT mice, or NHE2$^{-/-}$ mice. The latter strain did not react to DSS treatment differently than their genetically matched WT littermates, with the mortality curve tightly overlapping that of NHE3$^{+/+}$ animals (not shown). Upon macroscopic inspection, DSS-treated NHE3$^{-/-}$ mice

were found to show intestinal hemorrhage extending to the proximal small intestine (Fig. 4B–C), also confirmed by the haemoccult test. Pretreatment (10 days) followed by concurrent administration of DSS with ciprofloxacin and metronidazole, only delayed the body weight loss and mortality in NHE3$^{-/-}$ mice, which reached 100% on day 6. A similar delay was observed in mice injected with anti-ASGM1 antibodies prior to DSS administration (not shown).

DSS treated NHE3-deficient mice develop anemia and leukocytosis

For further studies on the effects of DSS, we chose a 48 hours time point, which is not sufficient to develop any symptoms in WT mice, but results in only relatively modest (~20%) mortality in NHE3$^{-/-}$ mice. Baseline hematological parameters did not differ between untreated WT and NHE3$^{-/-}$ mice. Similarly, within two days of DSS treatment, WT mice demonstrated no significant changes in the measured blood parameters (Fig. 5). Consistent with the observed intestinal bleeding, DSS-treated NHE3$^{-/-}$ mice had a dramatically lower erythrocyte count (Fig. 5A), hemoglobin, and hematocrit (not shown). Assuming 80 ml of blood per kg body weight in mice, the calculated average total blood loss (BL) in DSS-treated NHE3$^{-/-}$ mice [BL=[(Hb-MinimumHb)/Hb]x(Weight in kg) x (ml of blood per kg body weight)] amounted to 0.95 ml (59%) within 48 hrs of treatment. In human patients, this would be classified as a severe blood loss or class IV hemorrhage. The total white blood cell count was significantly elevated, with lymphocytes, neutrophils, monocytes, and to a lesser extent, eosinophils, contributing to this leukocytosis (Fig. 5B–F). In NHE3$^{-/-}$ mice reacting most severely to DSS based on their body weight loss, the hematologist blinded to the study design frequently observed bacteria on blood smears, indicating septicemia. Oral antibiotics and the anti-ASGM1 antibody partially reversed the effects of DSS treatment on intestinal bleeding and the drop in the red blood cell count (Fig. 5A), but remained without effect on leukocytosis (Fig. 5B–F). Similar effects were observed with orally administered iNOS inhibitor, aminoguanidine (not shown). While all three treatments delayed the mortality, they were not able to prevent the development of sepsis, and all knockout mice died within six days of DSS treatment.

DSS further alters small intestinal apical junction complexes and increases mucosal tracer flux in NHE3$^{-/-}$ mice

When the proportion of the dilated AJC's were estimated in the TEM images by an investigator blinded to the group/genotype designation, DSS treatment significantly increased the already elevated number of widened AJC's (Fig. 6A). NHE3$^{-/-}$ mice and their wild-type littermates were treated with water or 4% DSS for 48 hours and then gavaged with two fluorescently labeled markers of mucosal permeability, FITC-SA or FITC-dextran. In WT mice, 48hours 4% DSS treatment did not alter gut permeability to these two markers (Fig. 6B). Somewhat surprisingly, despite the observed morphological and immunohistochemical changes we have not observed an increased mucosal tracer flux in untreated NHE3$^{-/-}$ mice. This suggests the existence of a compensatory mechanism which may be sufficient to mitigate the mucosal permeability in the absence of epithelial injury. Contrary to the wild-type mice, DSS-treated NHE3$^{-/-}$ mice displayed a dramatic increase in sulfonic acid flux, and a moderate, but statistically significant increase in the flux of the larger marker, FITC-dextran (Fig. 6B). These increases are likely to be highly underestimated due to the loss of whole blood into the intestinal lumen.

NHE3 as a modifier gene in the small intestinal and colonic injury

For reasons that remain unclear, DSS does not normally affect small intestine. This generally well-known phenomenon was confirmed by the very limited changes in the small intestinal gene expression pattern in wild-type mice, where only 38 genes/probe sets were identified as affected by DSS treatment (Fig. 7A). Almost all of those genes were non-

informative unannotated IMAGE/RIKEN clones with no known function or homology. In NHE3$^{-/-}$ mice, however, we have identified 363 genes/probe sets dysregulated by a 48-hour DSS treatment. This number was even greater than what we observed in the colon [19] (Fig. 7A). While the number of colonic genes affected by DSS treatment was similar in NHE3-deficient mice and in their wild-type littermates, there was only a minimal overlap in the identity of the affected genes, with only 13 of them overlapping in both genotypes (Venn diagram in Fig. 7B).

Although no major histological changes in the jejunum of untreated NHE3-deficient mice have been reported (Ref. 18 and our own unpublished observations), DSS treatment altered the architecture of the ileal mucosa with detectable lymphocytic and granulocytic infiltration, and visible hyperemia with dilated submucosal blood vessels (Fig. 8). Within two days of DSS treatment, colonic morphology did not demonstrate inflammation exacerbated beyond that reported by our group earlier [19], while the effects of longer exposure could not be assessed due to very high mortality rates.

Discussion

Slc9a3 gene knockout originally described by Schultheiss et al.[17] provided the first evidence for the critical role of NHE3 in intestinal and renal electrolyte transport and in systemic acid/base balance. The same group demonstrated later that the NHE3 knockout mice overexpress IFN-γ and IFN-γ inducible genes in the small intestinal mucosa[18] and attributed this increase to a homeostatic response aimed at mitigating Cl^- secretion in the face of impaired transepithelial Na^+ absorption. The source of IFN-γ, the etiology of its induction, and its potential consequences have not been described to date. More recently, our group has demonstrated that conventionally housed NHE3$^{-/-}$ mice develop bacterially-mediated mild to moderate distal colitis amenable to antibiotic treatment[19]. These findings collectively suggest that the loss of intestinal NHE3 activity has significant consequences extending beyond impaired vectorial Na^+ transport. Such inhibition or loss of activity is not limited to genetically modified mice. NHE3 is a target for downregulation by microbial pathogens and proinflammatory cytokines which may affect NHE3 gene transcription or transporter activity. As such, its inhibition has been attributed to the pathogenesis of infectious diarrhea as well as in chronic idiopatic inflammatory bowel diseases. In a recent report, Sullivan et al.[14] demonstrated that among other transport-related genes, NHE3 (but not NHE2), and NHERF1 were downregulated in the sigmoid of patients with active ulcerative colitis (UC) and Crohn's disease (CD), and in the ileal biopsies of active CD. NHE3 was also decreased in about 50% of sigmoid biopsies from inactive UC or CD. Consistently, Siddique et al. showed that NHE3 activity and protein expression was reduced in treatment-naïve UC and CD patients and remained low after 5-ASA[13].

We confirmed that NHE3 deficiency leads not only to induction of IFN-γ and IFN-inducible genes, but that the transcriptional profile of the small intestinal mucosa is altered to an extend not appreciated previously. We identified genes consistent with mucosal infiltration by immune cells which were likely candidate sources of IFN-γ. These included TCRα, TCRγ, CD8α, CD3 polypeptides δ, ε, and γ and were accompanied by induction of a number of genes from the MHCI and II antigen presentation pathways, along with genes involved in leukocyte transendothelial migration, adhesion molecules, TLR-signaling, and apoptosis. Induction of granzymes A, B, and K is consistent with the activation of CD8α$^+$ T cells and/or NK cells into the NHE3$^{-/-}$ mucosa. Indeed, IEL and LPL mononuclear cells were not only increased in numbers in NHE3$^{-/-}$ mice, but they displayed markedly elevated expression of IFN-γ. Treatment with an immunodepleting antibody against ASGM1 returned the expression of IFN-γ and iNOS to baseline levels thus suggesting an involvement of NK cells and CD8α$^+$ ASGM1$^+$ memory T cells. Similarly, treatment of

NHE3-deficient mice with broad-spectrum antibiotics reduced the cytokine expression in the small intestinal mucosa suggesting an active, yet controlled immune response to microbial antigens. The specific nature of this response remains unclear, although it may be related to a primary microbial challenge earlier in the development. We routinely observe limited spontaneous mortality and morbidity in NHE3$^{-/-}$ mice at 2–4 weeks of age, a period of rapid post-weaning increase of NHE3 expression and activity in wild-type rodents [21]. In the majority of surviving mice, the symptoms (diarrhea, body weigh disparity) tend to improve later in life (unpublished data). It is therefore conceivable that the initial insult in NHE3$^{-/-}$ mice occurs in the early post-weaning period and may be sustained by an epithelial dysfunction.

The elevated IFN-γ, in addition to its potentially beneficial antisecretory effects[18] may also play a detrimental role through its negative effects on the epithelial barrier[22, 23]. Change of the cellular distribution of occludin and E-cadherin, along with decreased expression of β-actin mRNA and F-actin staining may all contribute to the changes in the appearance of the apical junction complexes as observed by TEM, and in general in the structural and signaling network determining epithelial cellular polarity and adhesion. Increased expression of claudin-2 in NHE3$^{-/-}$ mice may be considered as a compensatory response leading to an increased paracellular Na^+ flux. Claudin-2 has been shown to form relatively selective pores for monovalent cation conductance[24]. However, Na^+ flux through claudin-2 pore is bidirectional and gradient-driven, and the change of Na^+ flux to serosal-to-apical, may be at least partially responsible for inability of NHE3$^{-/-}$ mice to tolerate Na^+-depleted diet[25]. Importantly, upregulation of claudin-2 has been reported in IBD[26], leads to increased TJ permeability[27], and has been recently suggested to contribute to IBD-associated colon cancer[28]. Indeed, the loss of NHE3, increased claudin-2 and diminished E-cadherin may be viewed as elements of ongoing dedifferentiation related to epithelial restitution.

These preset changes in the intestinal epithelium of NHE3$^{-/-}$ mice may predispose them to a disproportionate response to chemically induced mucosal injury. In contrast to DSS-treated WT or NHE2 null knockout mice, NHE3$^{-/-}$ mice developed rapid wasting disease, rectal bleeding, and accelerated mortality reaching 100% on day five. This was observed even with low 0.5–1% DSS concentration normally ineffective in wild-type mice. Moreover, heterozygous mice also displayed an exacerbated response in terms of mortality rates, thus suggesting haploinsufficiency and a possibility that in clinical situations characterized by partial NHE3 inhibition, NHE3 may be a determinant of the extent of epithelial injury and/or restitution. The severely exacerbated phenotype of DSS-treated NHE3$^{-/-}$ mice was accompanied by increased paracellular permeability, small intestinal bleeding, severe anemia, and leukocytosis consistent with septicemia. Intestinal hemorrhage is likely to be secondary to changes in mucosal microcirculation affected by increased NO production and dramatically and paradoxically decreased expression of endothelin 1. This notion gains support from the hyperemia observed in H&E sections in the ileum of DSS-treated NHE3-deficient mice. Importantly, anti-ASGM1 or antibiotic treatment, which effectively down-regulated IFN-γ and iNOS in NHE3$^{-/-}$ mice, limited intestinal hemorrhage, but not the leukocytosis developed after DSS treatment. Furthermore, these treatments only delayed, but did not prevent the accelerated mortality, thus suggesting that while IFN-γ and iNOS may contribute to the exaggerated response to DSS, absence of functional NHE3 may result in an intrinsic defect in the intestinal epithelial cells.

DSS is known to preferentially affect the colon[29], and to our knowledge, this is the first report of such an extensive small intestinal reaction to DSS-mediated mucosal injury. Microarray analysis not only confirmed a significantly affected small intestinal transcriptome, but also demonstrated considerably different colonic reaction to DSS, with a very minor overlapping set of genes dysregulated by DSS treatment in wild-type and NHE3-

deficient mice. These findings strongly suggest that NHE3 activity may serve as a factor determining the extent and severity of reaction to mucosal injury in the face of a pathogenic challenge or in the immune-mediated tissue damage in IBD.

Several factors may contribute to the observed DSS susceptibility, including cellular stress due to metabolic adaptations to the diminished Na^+/H^+ exchange, alterations in bacterial-epithelial interactions[19], or changes in intracellular, organellar, and/or microenvironmental pH. Changes to paracellular permeability are influenced by variations of the extracellular pH, and recent studies with molecular and atomic force spectroscopy clearly demonstrate that overall adhesion strength of tight junction proteins is affected by the environment's pH[30]. Moreover, induction of the electrogenic transepithelial Na^+ transport with aldosterone results in tightening of the epithelial barrier[31], and it is conceivable, that the electroneutral Na^+ transport has a similar effect.

Conclusions

The effects of the NHE3 deficiency on the intestinal epithelium and in the described susceptibility to mucosal injury are complex and likely multifactorial. Our findings not only provide first evidence of such involvement, but also open an unexplored avenue to investigate the involvement of NHE3-mediated Na^+/H^+ exchange mechanism in the gut epithelial cell homeostasis.

Supplementary Material

Refer to Web version on PubMed Central for supplementary material.

Acknowledgments

Grant support: NIH 2R01DK041274 (to F.K.G.)

Abbreviations

NHE3	Na^+/H^+ exchanger 3
DSS	dextran sulfate sodium
IEL	intraepithelial lymphocytes
LPL	lamina propria lymphocytes
NK	natural killer cells
ASGM1	asialo GM1
iNOS	NOS2, inducible nitric oxide synthase
NO	nitric oxide
PMA	phorbol 12-myristate 13-acetate

References

1. Seidler U, Lenzen H, Cinar A, et al. Molecular mechanisms of disturbed electrolyte transport in intestinal inflammation. Ann N Y Acad Sci. 2006; 1072:262–75. [PubMed: 17057206]
2. Pardi DS. Microscopic colitis: an update. Inflamm Bowel Dis. 2004; 10:860–70. [PubMed: 15626904]
3. Hawker PC, McKay JS, Turnberg LA. Electrolyte transport across colonic mucosa from patients with inflammatory bowel disease. Gastroenterology. 1980; 79:508–11. [PubMed: 7429111]

4. Allan R, Steinberg DM, Dixon K, et al. Changes in the bidirectional sodium flux across the intestinal mucosa in Crohn's disease. Gut. 1975; 16:201–4. [PubMed: 1123174]
5. Sandle GI, Hayslett JP, Binder HJ. Effect of glucocorticoids on rectal transport in normal subjects and patients with ulcerative colitis. Gut. 1986; 27:309–16. [PubMed: 3699552]
6. Clayburgh DR, Musch MW, Leitges M, et al. Coordinated epithelial NHE3 inhibition and barrier dysfunction are required for TNF-mediated diarrhea in vivo. J Clin Invest. 2006; 116:2682–94. [PubMed: 17016558]
7. Musch MW, Clarke LL, Mamah D, et al. T cell activation causes diarrhea by increasing intestinal permeability and inhibiting epithelial Na+/K+-ATPase. J Clin Invest. 2002; 110:1739–47. [PubMed: 12464679]
8. Rocha F, Musch MW, Lishanskiy L, et al. IFN-gamma downregulates expression of Na(+)/H(+) exchangers NHE2 and NHE3 in rat intestine and human Caco-2/bbe cells. Am J Physiol Cell Physiol. 2001; 280:C1224–32. [PubMed: 11287336]
9. Amin MR, Malakooti J, Sandoval R, et al. IFN-gamma and TNF-alpha regulate human NHE3 gene expression by modulating the Sp family transcription factors in human intestinal epithelial cell line C2BBe1. Am J Physiol Cell Physiol. 2006; 291:C887–96. [PubMed: 16760259]
10. Kiela PR, Guner YS, Xu H, et al. Age- and tissue-specific induction of NHE3 by glucocorticoids in the rat small intestine. Am J Physiol Cell Physiol. 2000; 278:C629–37. [PubMed: 10751311]
11. Yun CC, Chen Y, Lang F. Glucocorticoid activation of Na(+)/H(+) exchanger isoform 3 revisited. The roles of SGK1 and NHERF2. J Biol Chem. 2002; 277:7676–83. [PubMed: 11751930]
12. Kiela PR, Hines ER, Collins JF, et al. Regulation of the rat NHE3 gene promoter by sodium butyrate. Am J Physiol Gastrointest Liver Physiol. 2001; 281:G947–56. [PubMed: 11557515]
13. Siddique I, Hasan F, Khan I. Suppression of Na(+)/H(+) exchanger isoform-3 in human inflammatory bowel disease: Lack of reversal by 5′-aminosalicylate treatment. Scand J Gastroenterol. 2008:1–9.
14. Sullivan S, Alex P, Dassopoulos T, et al. Downregulation of sodium transporters and NHERF proteins in IBD patients and mouse colitis models: Potential contributors to IBD-associated diarrhea. Inflamm Bowel Dis. 2008
15. Hayashi H, Szaszi K, Coady-Osberg N, et al. Inhibition and redistribution of NHE3, the apical Na +/H+ exchanger, by Clostridium difficile toxin B. J Gen Physiol. 2004; 123:491–504. [PubMed: 15078917]
16. Hecht G, Hodges K, Gill RK, et al. Differential regulation of Na+/H+ exchange isoform activities by enteropathogenic E. coli in human intestinal epithelial cells. Am J Physiol Gastrointest Liver Physiol. 2004; 287:G370–8. [PubMed: 15075254]
17. Schultheis PJ, Clarke LL, Meneton P, et al. Renal and intestinal absorptive defects in mice lacking the NHE3 Na+/H+ exchanger. Nat Genet. 1998; 19:282–5. [PubMed: 9662405]
18. Woo AL, Gildea LA, Tack LM, et al. In vivo evidence for interferon-gamma-mediated homeostatic mechanisms in small intestine of the NHE3 Na+/H+ exchanger knockout model of congenital diarrhea. J Biol Chem. 2002; 277:49036–46. [PubMed: 12370192]
19. Laubitz D, Larmonier CB, Bai A, et al. Colonic gene expression profile in NHE3-deficient mice: evidence for spontaneous distal colitis. Am J Physiol Gastrointest Liver Physiol. 2008; 295:G63–G77. [PubMed: 18467500]
20. Kosaka A, Wakita D, Matsubara N, et al. AsialoGM1+CD8+ central memory-type T cells in unimmunized mice as novel immunomodulator of IFN-gamma-dependent type 1 immunity. Int Immunol. 2007; 19:249–56. [PubMed: 17229818]
21. Collins JF, Xu H, Kiela PR, et al. Functional and molecular characterization of NHE3 expression during ontogeny in rat jejunal epithelium. Am J Physiol. 1997; 273:C1937–46. [PubMed: 9435499]
22. Bruewer M, Samarin S, Nusrat A. Inflammatory bowel disease and the apical junctional complex. Ann N Y Acad Sci. 2006; 1072:242–52. [PubMed: 17057204]
23. Chiba H, Kojima T, Osanai M, et al. The significance of interferon-gamma-triggered internalization of tight-junction proteins in inflammatory bowel disease. Sci STKE. 2006:pe1. [PubMed: 16391178]

24. Yu AS, Cheng MH, Angelow S, et al. Molecular basis for cation selectivity in claudin-2-based paracellular pores: identification of an electrostatic interaction site. J Gen Physiol. 2009; 133:111–27. [PubMed: 19114638]
25. Ledoussal C, Lorenz JN, Nieman ML, et al. Renal salt wasting in mice lacking NHE3 Na+/H+ exchanger but not in mice lacking NHE2. Am J Physiol Renal Physiol. 2001; 281:F718–27. [PubMed: 11553519]
26. Mankertz J, Schulzke JD. Altered permeability in inflammatory bowel disease: pathophysiology and clinical implications. Curr Opin Gastroenterol. 2007; 23:379–83. [PubMed: 17545772]
27. Hou J, Gomes AS, Paul DL, et al. Study of claudin function by RNA interference. J Biol Chem. 2006; 281:36117–23. [PubMed: 17018523]
28. Weber CR, Nalle SC, Tretiakova M, et al. Claudin-1 and claudin-2 expression is elevated in inflammatory bowel disease and may contribute to early neoplastic transformation. Lab Invest. 2008; 88:1110–20. [PubMed: 18711353]
29. Okayasu I, Hatakeyama S, Yamada M, et al. A novel method in the induction of reliable experimental acute and chronic ulcerative colitis in mice. Gastroenterology. 1990; 98:694–702. [PubMed: 1688816]
30. Lim TS, Vedula SR, Hui S, et al. Probing effects of pH change on dynamic response of Claudin-2 mediated adhesion using single molecule force spectroscopy. Exp Cell Res. 2008; 314:2643–51. [PubMed: 18602630]
31. Amasheh S, Milatz S, Krug SM, et al. Na+ absorption defends from paracellular back-leakage by claudin-8 upregulation. Biochem Biophys Res Commun. 2009; 378:45–50. [PubMed: 19000657]
32. Schultheis PJ, Clarke LL, Meneton P, et al. Targeted disruption of the murine Na+/H+ exchanger isoform 2 gene causes reduced viability of gastric parietal cells and loss of net acid secretion. J Clin Invest. 1998; 101:1243–53. [PubMed: 9502765]
33. Ni J, Chen SF, Hollander D. Immunological abnormality in C3H/HeJ mice with heritable inflammatory bowel disease. Cell Immunol. 1996; 169:7–15. [PubMed: 8612297]

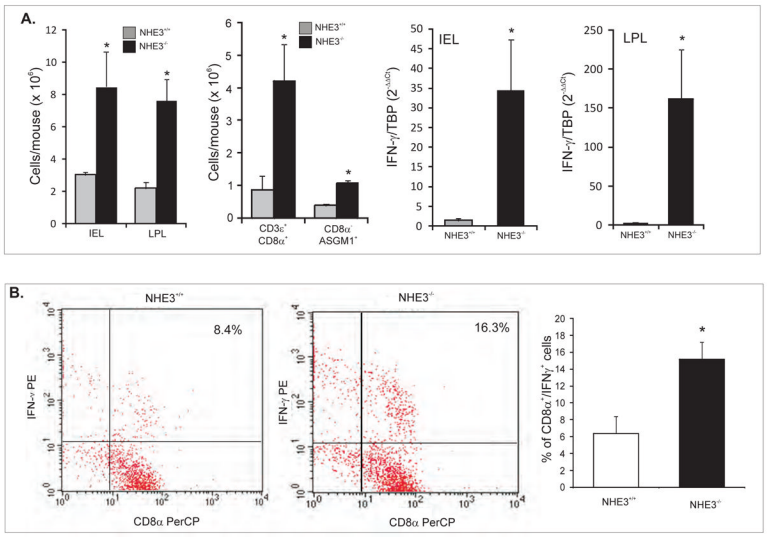

Figure 1. The source(s) of IFN-γ in the small intestinal mucosa of NHE3$^{-/-}$ mice

(**A**) Yields of intraepithelial (IEL) and lamina propria (LPL) mononuclear cells, and LPL CD8α^{+} or CD8α^{-}ASGM1^{+} cells isolated from the small intestine of WT and NHE3$^{-/-}$ mice, and real-time PCR analysis of IFN-γ mRNA expression in IEL and LPL cells from WT and NHE3$^{-/-}$ mice. (**B**) Flow cytometry analysis of intracellular IFN-γ in magnetically sorted CD8α^{+} cells stimulated in vitro with PMA and ionomycin in the presence of brefeldin A. Bar graph depicts summary of four independent experiments.

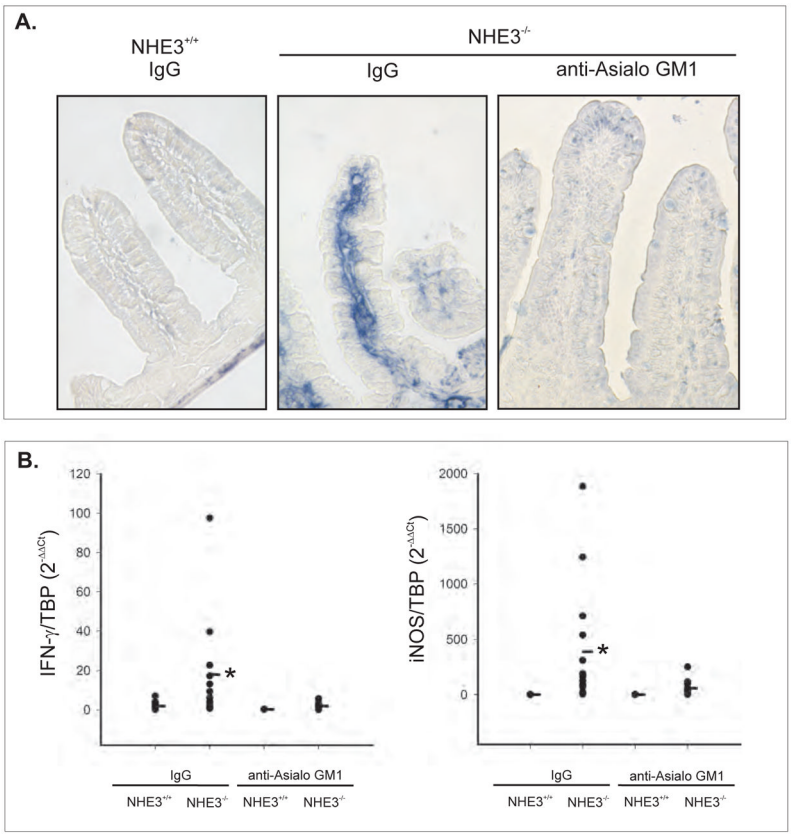

Figure 2. The source(s) of IFN-γ in the small intestinal mucosa of NHE3$^{-/-}$ mice

(**A**) I*n situ* hybridization for IFN-γ mRNA in WT mice treated with control IgG or in NHE3$^{-/-}$ mice treated with IgG or anti-asialo GM1 antibodies. (**B**) Real-time PCR analysis of IFN-γ and iNOS mRNA expression in the small intestinal mucosa of WT and NHE3$^{-/-}$ mice treated with IgG or anti-ASGM1 antibodies. * significant differences between WT and NHE3$^{-/-}$ mice [ANOVA followed by post hoc Fisher's protected least significant difference (PLSD) test, $p<0.05$; n=3–14]

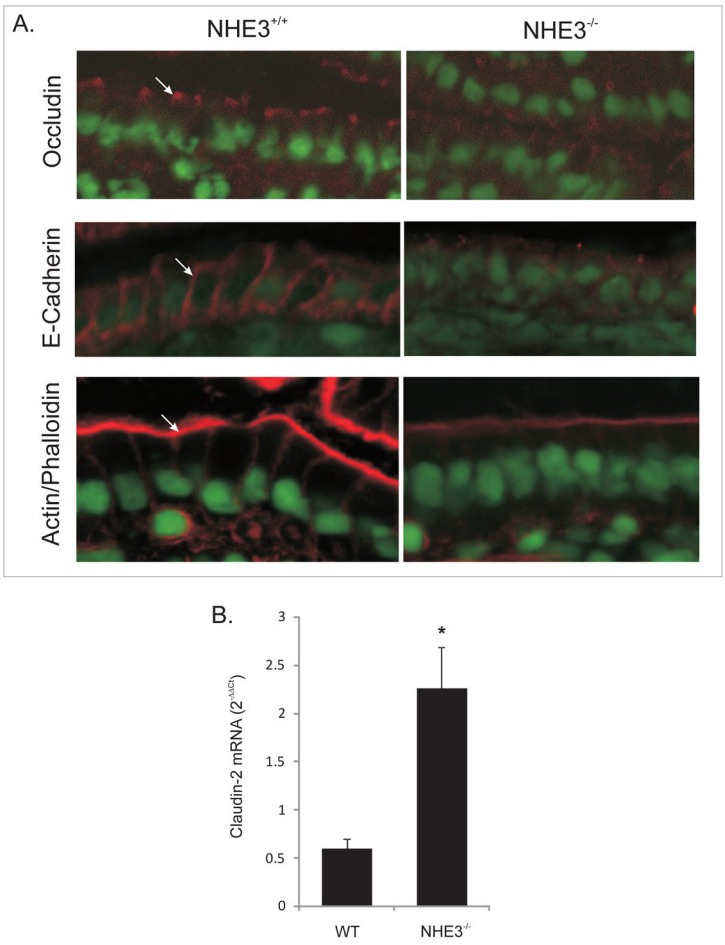

Figure 3AB.

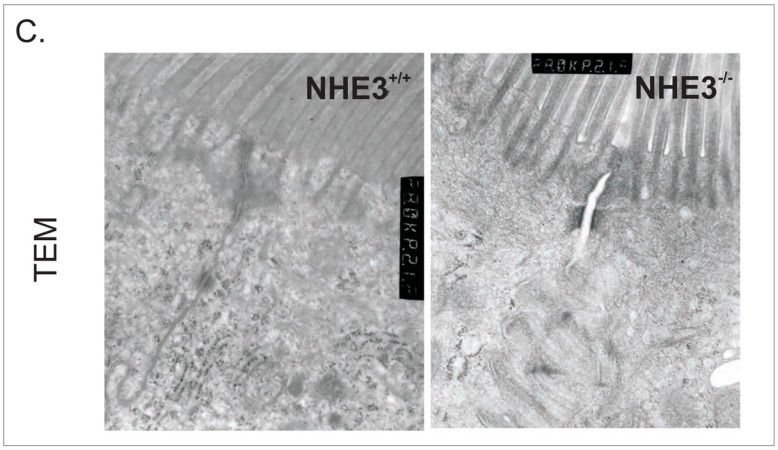

Figure 3C.

Figure 3.

(**A**) Immunohistochemical analysis of occludin, E-cadherin, and phalloidin staining of polymerized F-actin in the small intestinal epithelium of WT and NHE3$^{-/-}$mice. (**B**) Real-

time RT-PCR analysis of claudin-2 expression in the mucosa of WT and NHE3$^{-/-}$ mice. (**C**) Representative TEM image of the apical junction complex area in the epithelium of WT and NHE3$^{-/-}$ mice.

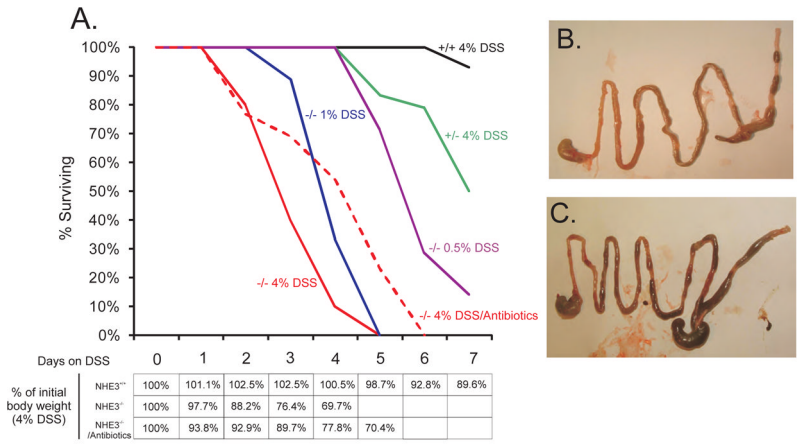

Figure 4. Dramatic effects of DSS in NHE3-deficient mice

(**A**) Mortality of NHE3$^{+/+}$, NHE3$^{+/-}$, and NHE3$^{-/-}$ mice in response to DSS. Red dashed line represents mortality rates in NHE3$^{-/-}$ mice treated with 4% DSS and ciprofloxacin and metronidazole. Table depicts body weight loss in WT and NHE3$^{-/-}$ mice treated with 4% DSS with or without antibiotics. Gross intestinal morphology in WT (**B**) and NHE3$^{-/-}$ mice (**C**) treated with 4% DSS for 48 hrs. Visible thickening of the colonic wall and intestinal hemorrhage extending into the proximal small intestine in NHE3$^{-/-}$ mice.

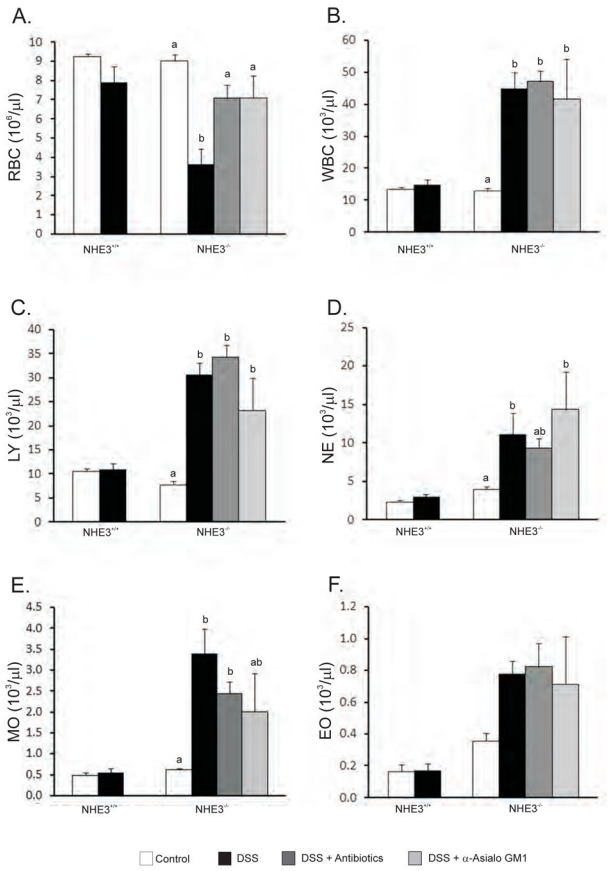

Figure 5. Hematology analysis

(**A**) Red blood cell (RBC) count, (**B**) white blood cell (WBC) count, (**C**) lymphocyte (LY) count, (**D**) neutrophil (NE) count, (**E**) monocytes (MO), and (**F**) eosinophils (EO). No statistical differences were observed in control and DSS treated WT mice. Antibiotics or control IgG were without effect in WT mice and were omitted from the graph for clarity. Data from NHE3$^{-/-}$ mice were analyzed with ANOVA followed by post hoc Fisher's protected least significant difference test, with $P \leq 0.05$ considered significant and depicted as different letters next to bars.

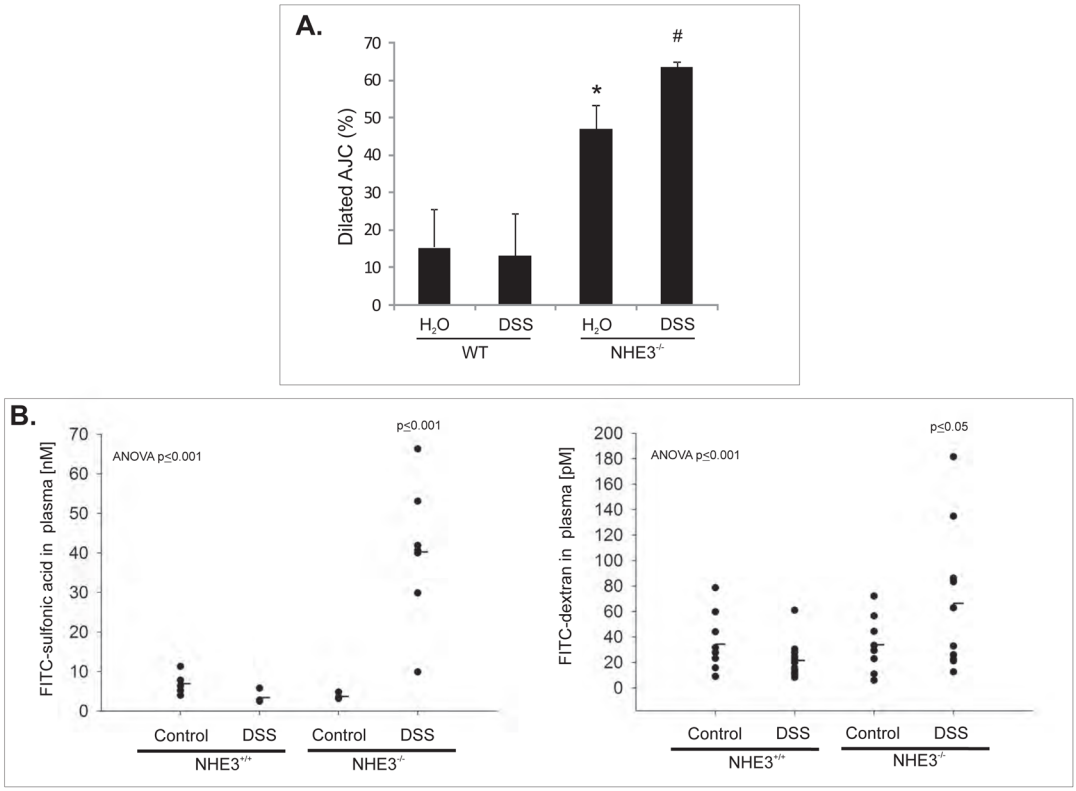

Figure 6.

(A) *Quantitative summary of the TEM analysis of the apical junction complex(AJC) in the small intestinal epithelium of untreated and DSS-treated WT and NHE3*$^{-/-}$ *mice.* Mice were treated with 4% DSS for 48 hrs. 30–40 AJC's per specimen were analyzed and designated as dilated or not. Average percent contribution of dilated AJC's was calculated and statistically analyzed by ANOVA followed by post hoc Fisher's PLSD test, with $P \leq 0.05$ considered significant and depicted as different symbols next to bars (n=4). (**B**) *Intestinal mucosal tracer flux in untreated and DSS-treated WT and NHE3*$^{-/-}$ *mice.* Mice were treated with DSS as above and then gavaged with FITC-SA or FITC-dextran as described in the Supplementary Methods section. Marker-associated fluorescence was measured in blood plasma and concentrations calculated from respective standard curve. The results were statistically analyzed by ANOVA followed by post hoc Fisher's protected least significant difference test, with $P \leq 0.05$ considered significant and depicted by the p values. Only DSS-treated NHE3$^{-/-}$ mice were different from other groups (n=5–10).

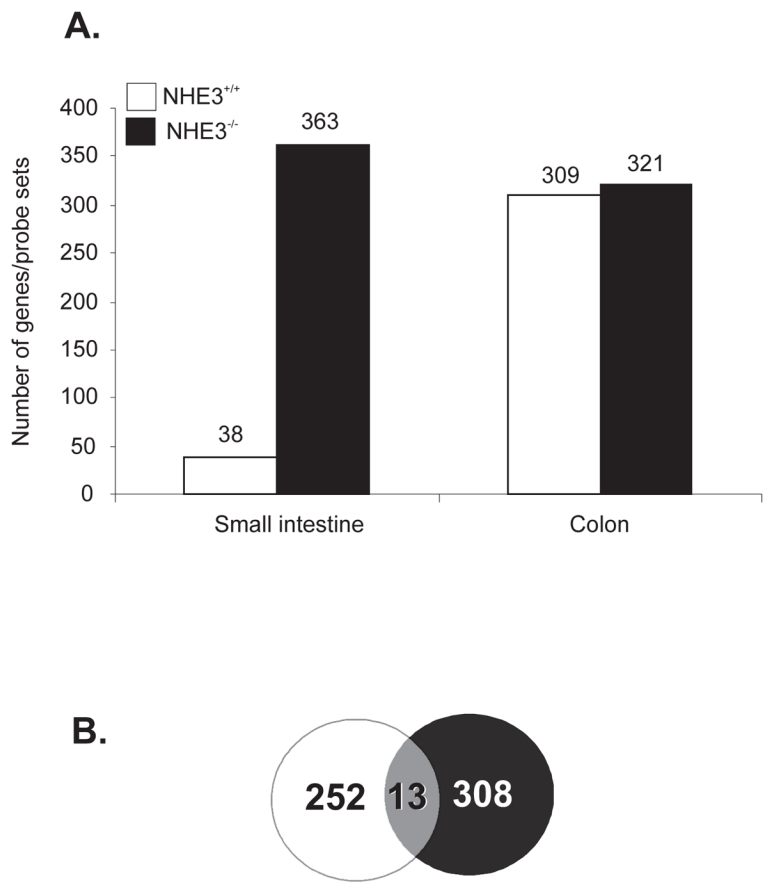

Figure 7. Comparative microarray analysis of small intestinal and colonic gene expression profiles of untreated and DSS-treated WT and NHE3$^{-/-}$ mice

Mice were treated with water or 4% DSS for 48 hrs and small intestinal and colonic gene expression profile was analyzed with Mouse Genome 430 2.0 arrays (Affymetrix) and Gene Spring software (Agilent) as described in the Materials and Methods section. (**A**) Number of genes/probe sets induced or repressed ≥2 fold ($p<0.05$, t-test) in the small intestinal or colonic mucosa in WT (open bars) and NHE3$^{-/-}$ mice (black bars). (**B**) Venn diagram depicting very limited overlap in the sets of genes regulated by DSS in the colon of WT and NHE3$^{-/-}$ mice. The depicted number of overlapping genes was reduced from 57 to 13 to visualize only functionally annotated genes in this group of probe sets.

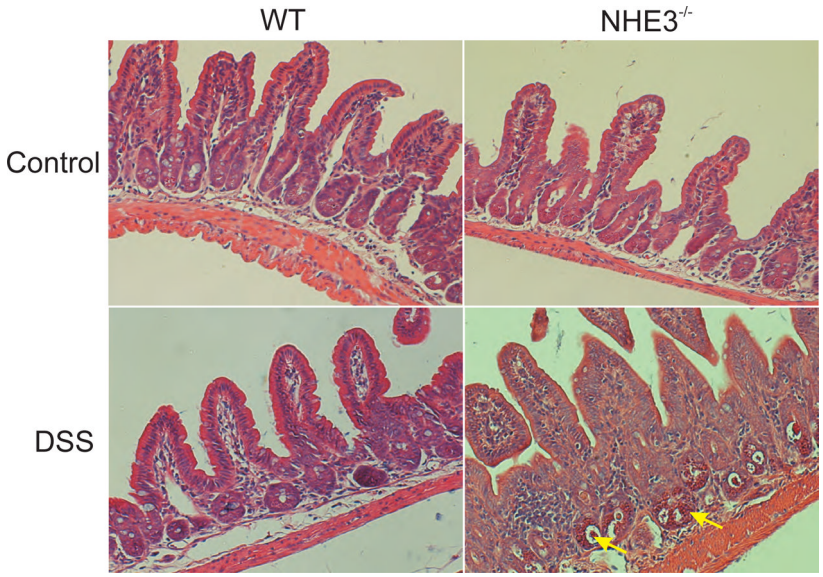

Figure 8. Histological evaluation of ileal mucosal morphology of untreated and DSS-treated WT and NHE3$^{-/-}$ mice

Mice were treated with 4% DSS for 48 hrs. Representative H&E-stained sections of distal ileum demonstrate no noticeable changes in the ileal histology of untreated WT and NHE3$^{-/-}$ mice, or DSS-treated WT mice, whereas DSS-treated NHE3$^{-/-}$ mice displayed easily discernable neutrophilic and lymphocytic lamina propria infiltration and hyperemia (exemplified by yellow arrows).